# Structural Studies of Sugar Binding Proteins

Sanjeewani Sooriyaarachchi

*Faculty of Natural Resources and Agricultural Sciences*
*Department of Molecular Biology*
*Uppsala*

Doctoral Thesis
Swedish University of Agricultural Sciences
Uppsala 2010

Cover illustration: Ribbon cartoon of the closed xylose binding protein crystal structure (PDB entry 3MA0) from *Escherichia coli* in complex with xylose (by Sanjeewani Sooriyaarachchi).

Structural Studies of Sugar Binding Proteins

Abstract
Binding proteins, which are themselves non-enzymatic, play an important role in enzymatic reactions as well as non-enzymatic processes by providing a binding platform for the specific recognition of particular molecules. For example, periplasmic binding proteins play a vital role in nutrient uptake in Gram-negative bacteria.

In the present study, three sugar binding proteins, including two periplasmic binding proteins and a β-glucan binding protein, are described.

The glucose/galactose binding protein in complex with (2R)-glyceryl-β-D-galactopyranoside, another physiologically relevant ligand for the protein, was revealed. The structure was solved using the molecular replacement method and refined to 1.87 Å with R and R free values 17% and 22%. The structure displays the closest form among the available glucose/galactose binding protein structures with three additional binding residues, which are conserved among the group. We also present three different conformations of *E. coli* xylose binding protein structures, open ligand free, open liganded and closed liganded. This is the first structure of the open liganded form in the pentose/hexose sugar-binding cluster. The structures were solved using molecular replacement method and refined to 2.15 Å, 2.1 Å and to 2.2 Å respectively.

The new family of antimicrobial protein, secreted upon fungal attacks from *Pinus sylvestris* was present here with the binding and activity assays. The inhibition of vegetative growth and the spore germination of the causative agent of the disease, root and butt rot was proved with low concentrations of the peptide. The assays determined its ability to bind with β-(1,3)-D-glucans. The homology model was made using the PDB structure 1C01, the antimicrobial protein from *Macadamia integrifolia,* which has 64% sequence identity.

*Keywords:* antimicrobial protein, binding proteins, conformation, (2R)-glyceryl-β-D-galactopyranoside, β-(1,3)-D-glucan, homology modeling, X-ray structures, xylose

*Author's address:* Sanjeewani Sooriyaarachchi, SLU, Department of Molecular Biology, P.O. Box 590, Biomedical Centre, 75124, Uppsala, Sweden
*E-mail:* sanju@xray.bmc.uu.se

# Dedication

To my parents…
    for being my inspiration…


පිදුම.........
ආදරණීය අම්මාට හා තාත්තාට !

Contents

# List of Publications

This thesis is based on the work contained in the following papers, referred to by Roman numerals in the text:

I **Sooriyaarachchi, S**., Ubhayasekera, W., Boos, W. & Mowbray, S.L. (2009). X-ray structure of glucose/galactose receptor from *Salmonella typhimurium* in complex with the physiological ligand, (2R)-glyceryl-β-D-galactopyranoside. FEBS J 276(7), 2116-24.

II **Sooriyaarachchi, S.**, Ubhayasekera, W., Park, C., Mowbray, S.L. Conformational changes and ligand recognition of *Escherichia coli* D-xylose binding protein revealed. Submitted to *Journal of Molecular Biology*.

III **Sooriyaarachchi, S.★**, Jaber, E.★, Suárez Covarrubias, A., Ubhayasekera, W., Asiegbu, F. O., Mowbray, S.L. Scots pine antimicrobial proteins act by binding β-glucan (manuscript).

Papers I is reproduced with the permission of the publisher.
★ First authorship shared

# Abbreviations

| | |
|---|---|
| ABC | ATP binding cassette |
| AMP | antimicrobial peptides |
| ALBP | allose binding protein |
| ESRF | European Synchrotron Radiation Facility |
| GBP | glucose/galactose binding protein |
| GGal | (2R)-glyceryl-β-D-galactopyranoside |
| HEPES | 4-(2-hydroxyethyl)-1-piperazineethane-sulfonate |
| MeGal | methylgalactoside |
| PBP | periplasmic binding protein |
| PDB | Protein Data Bank |
| PEG | polyethylene glycol |
| PR | pathogenesis related protein |
| RBP | ribose binding protein |
| r.m.s. | root mean square |
| SAR | systemic acquired resistance |
| SCOP | structural classification of proteins |
| Sp-AMP | Scots pine antimicrobial peptide |
| UDP | uridine diphosphate |
| XBP | xylose binding protein |
| XBP-opn | open ligand free structure of xylose binding protein |
| XBP-opn-xyl | open liganded structure of xylose binding protein |
| XBP-cls-xyl | close liganded structure of xylose binding protein |

# 1 Introduction

## 1.1 Binding proteins

Binding proteins, which are essentially non-enzymatic, plays an important role in enzymatic reactions as well as non-enzymatic processes by providing a binding platform for substrates, either endogenous or exogenous. A specific affinity to its ligand is a common feature of all binding proteins. For example, most of the known carbohydrate-degrading enzymes contain two or more modules, one for catalysis (the catalytic module) and the rest for substrate binding, e.g. the carbohydrate binding modules of cellulases (Arai *et al*., 2003), chitinases (Arakane *et al*., 2003) and β-1,4 glycanases (Gilkes *et al*., 1991). The binding module serves as an anchor, promoting the enzymatic activity by keeping the catalytic module closer to the substrate. The activity of the catalytic module is usually independent from the substrate-binding module. However, the two modules together would have the maximum rate of enzyme reaction on solid substrates.

Most of the antimicrobial proteins investigated so far have been categorized as binding proteins ((e.g. hevein and knottin type antimicrobial peptides (Iseli *et al*., 1993; Raikhel *et al*., 1993)), and most of them are sugar binding proteins. In the transport machinery in living cells, binding proteins also play a vital role, especially in bacteria. Periplasmic binding proteins (PBPs) serve as non-enzymatic components of ATP binding cassette (ABC) transport systems.

In this thesis I have presented two periplasmic sugar binding proteins, which direct the sugar molecules to be transported *via* ABC transport systems, and one antimicrobial protein, which binds to the fungal cell wall, and destroys it.

# 2 Background

## 2.1 Cargo into and out from the cell

### 2.1.1 Bacterial transport systems

The cytosol is a translucent fluid that contains a mixture of soluble materials such as sugars, fatty acids, amino acids, many enzymes and co-enzymes, vitamins etc. Cell membrane prevents diffusion of all these materials to the outside less concentrated environment, compared to the inside of the cell. Therefore, transportation of nutrients and other required substances into the cell, as well as efflux of the waste products out, are key cellular events, and different machineries have evolved for these processes.

The transport systems in prokaryotes can be classified as simple transport, group translocation and ABC systems. In simple transport, the substrate is carried across the cell membrane without being chemically altered. The transport is driven by energy from the proton motive force. There are three different types of simple transport events, performed by uniporters, antiporters and symporters. Lac permease is one well-known example of a simple transport system. In group translocation, several specific and non-specific enzymes are involved in the transport process. In one example, sequential phosphate transfer occurs while transporting the substance, which would chemically altered during its passage across the membrane. Energy for the transport process comes from the energy-rich compound phosphoenolpyruvate.
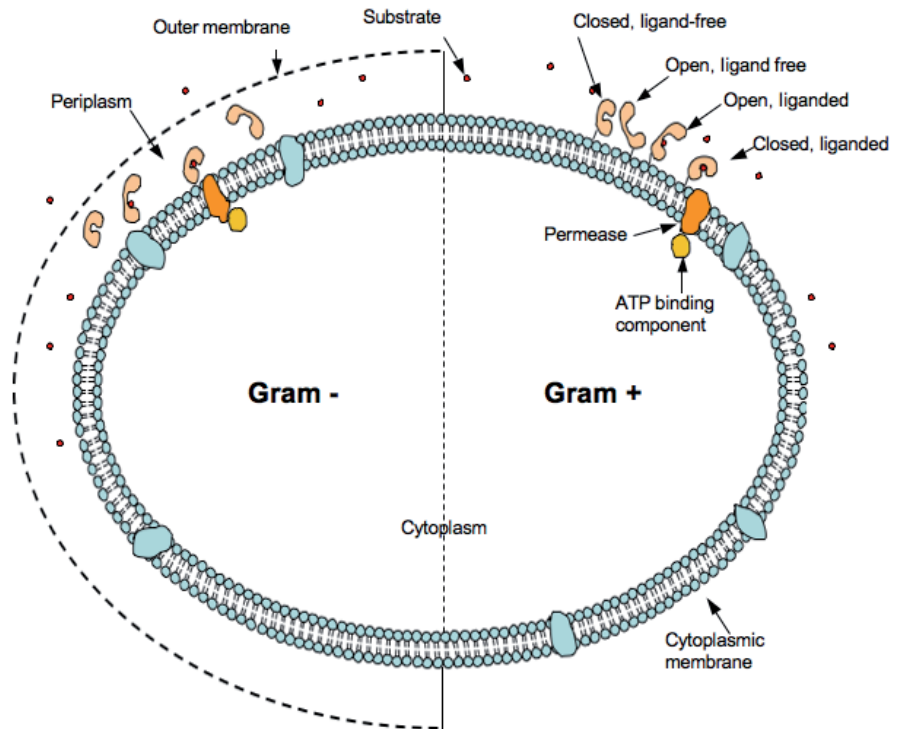
*Figure 1.* A schematic diagram showing the arrangement of the cell wall and the ABC transport systems in Gram–negative and –positive bacteria.

### 2.1.2 ABC transport systems

ABC transport systems are common in all living organisms, including archea, eubacteria and eukaryotes (Higgins, 1992). In bacteria, the system consists of three major components (see Fig. 1): the periplasmic (or equivalent) binding component, two integral membrane domains each with six segments that span the membrane, and two ATP hydrolyzing domains. The ATP domain is the most conserved part, while the membrane integral component is less conserved. The periplasmic binding component is the most divergent, and the best-studied, part of this transport system. ABC transport systems are involved in both export and import. Such systems are also responsible for several other types of events, including protein secretion, drug and antibiotic resistance, signal transduction, antigen presentation, bacterial pathogenesis and sporulation (Higgins, 1992).

### 2.1.3 Periplasmic binding component superfamily

A bacterial cell is separated from its outside environment by the cytoplasmic membrane, which is a highly selective semi-permeable barrier. Bacteria must take up all the great variety of necessary nutrients, like sugars, amino acids, vitamins, ions etc. from their surroundings through the cytoplasmic membrane in order to survive. At the same time, it is important to possess a selective mechanism or filtering system to avoid entry of unnecessary substances through the membrane. Special transport systems have evolved fulfilling all these requirements, allowing microbes to fit into the environment in which they live.

Periplasmic binding proteins (PBPs) are a vital part of the ABC transport systems, and are located in the periplasm, (Fig. 1) in-between the outer and inner membranes of the Gram-negative bacteria. PBPs are non-enzymatic receptors that are mainly involved in solute transport through the cell membrane, although many of them are also capable of acting as chemoreceptors by inducing chemotaxis towards the nutrient source (Higgins *et al.*, 1990; Tam & Saier, 1993). These proteins are highly water-soluble (Boos, 1974). Unlike membrane-integral proteins, PBPs display more stable behavior and solubility. Many PBPs unusually stable to heat and proteolytic digestion (Ames *et al.*, 1984). These reasons have led to PBPs being the best-studied proteins of the bacterial transport systems.

The cytoplasm is rich and dense in solutes compared to the outer environment. Therefore, passive diffusion of solutes in, through the cell membrane is not likely to take place. The low concentration of these solutes is itself the rate-limiting factor for transport. In such a case, the high affinity of a periplasmic binding component allows it to capture the solute molecules and direct them to the membrane-integral component. This process plays a primary role in enhancing the rate of entry of solute to cytosol through the membrane. Since bacteria live in environments where food is often limiting, this sort of system is necessary for their survival.

Gram-positive bacteria are surrounded by a single membrane, and thus do not have a periplasmic space (Fig. 1). In this case, the periplasmic binding component has been replaced by a membrane bound lipoprotein, which can act similarly to the periplasmic binding component in Gram-negative bacteria (Gilson *et al.*, 1988). However, the lipoprotein cannot move as freely as a periplasmic binding component, as it is tethered to the cell membrane to prevent it diffusing away from the cell (Fig.1).

It is obvious that the binding component is indispensable to increase the uptake efficiency. Living in highly chemically fluctuating environments

bacteria has the utmost importance of PBPs for gather the traces of nutrients needed for the survival.

Maltose transport in the absence of maltose binding protein (MBP) raises the question of the functional role of PBPs (Shuman, 1982). The functional necessity of the periplasmic binding component for the ABC transport system is obscure in the higher organisms. However, sequence analysis revealed that the diverse mammalian receptors contain extra cellular ligand binding domains that are homologous to the PBPs such as G protein-coupled receptors glutamate/glycine-gated ion channels (Nakanishi *et al.*, 1990).

Known PBPs have been categorized into eight main clusters (Tam & Saier, 1993) as listed below:
  i.      Binding proteins specific for malto-oligosacharides, multiple sugars, alpha-glycerol phosphate and iron
  ii.     Binding proteins specific for hexoses and pentoses
  iii.    Binding proteins specific for polar amino acids and opines
  iv.     Binding proteins specific for aliphatic amino acids and amides
  v.      Binding proteins specific for peptides and nickel
  vi.     Binding proteins specific for inorganic polyanions
  vii.    Binding proteins specific for organic polyanions
  viii.   Binding proteins specific for iron complexes and vitamin $B_{12}$

Proteins that share a common evolutionary origin share structural similarities. Making use of this knowledge of the relationships, a systematic structural classification of proteins (SCOP) has been attempted (Murzin *et al.*, 1995). The major levels of the hierarchy are family, superfamily and fold. Periplasmic binding proteins are categorized into two superfamilies, designated as periplasmic binding protein-like I and II. All the pentose and hexose binding proteins are assigned to the periplasmic binding protein-like I superfamily.

A number of structures for ligand free and ligand bound PBPs are available in the Protein Data Bank (PDB). The general PBP structure has the shape of a prolate ellipsoid, with two distinct lobes designated as the N- and C-terminal domains. Each domain is built up of two separate polypeptide segments, with the largest being drawn from the N and C halves of the amino acid chain, respectively, for the two domains. The C-terminal domain is generally significantly larger. The two domains are connected to each other by a two- or three- stranded hinge region. The hinge strands are spatially close to each other and demarcate the boundary of the ligand-binding pocket, which itself is located in the domain interface.

The two domains display a similar super-secondary structure, consisting of a central β-pleated sheet flanked by either side by helices (Quiocho, 1990; Davidson *et al.*, 2008).

### 2.1.4 Different conformations of PBPs

Structures of PBPs are available in open unliganded, open liganded, closed unliganded and closed liganded forms. The conformational changes take place upon ligand binding. The domains of the ligand free structures are well separated and water can freely enter to the ligand-binding pocket. Both domains participate in the ligand binding in the closed liganded structures, and the bound ligands are completely buried and separated from the bulk solvent.

Among the above-mentioned clusters (Tam & Saier, 1993), the hexose and pentose sugar binding proteins have been studied extensively. Glucose/galactose, ribose and allose binding protein structures are available in both open and closed conformations (Quiocho & Vyas, 1984; Vyas *et al.*, 1988; Mowbray *et al.*, 1990; Zou *et al.*, 1993; Flocco & Mowbray, 1994; Chaudhuri *et al.*, 1999; Borrok *et al.*, 2007; Cuneo *et al.*, 2008a). The glucose/galactose binding protein (Flocco & Mowbray, 1994) is the only available ligand free closed structure so far. The individual proteins display specificity to a narrow range of ligands (i.e. glucose and galactose, or leucine, isoleucine and valine). Although the structures display a similar fold and sometimes a similar pattern of binding, the sequence similarity among them is usually very low.

In the absence of substrate PBPs prefer to be in the open form, and in the presence of substrates they prefer the closed form. However, according to the multiple open conformations of available crystal structures suggest that ligand binding is not necessarily promoted the opening and closing of the PBPs. The three different open conformations of ribose binding protein (RBP, (Bjorkman & Mowbray, 1998)), allose binding protein (ALBP, (Magnusson *et al.*, 2002)), the liganded open form of leucine, isoleucine and valine (LIVBP,(Sack *et al.*, 1989)), and XBP liganded open structure from this study are the best available evidences for this. The available closed unliganded form further suggests that these proteins are in equilibrium as open and closed at least to some extent (Flocco & Mowbray, 1994) and this has been further confirmed by NMR studies (Tang *et al.*, 2007).

The available structures with multiple open conformations make it easier to picture the trajectory of the conformational change associated with ligand binding. The movement of the domains is primarily centered in the hinge region, which is flexible. The three open conformations observed for RBP

and ALBP showed that there is in each case a defined trajectory of the bending movement (Bjorkman & Mowbray, 1998; Magnusson *et al.*, 2002). However, although these PBPs show a similar structural fold, the direction and rotation of domain movements for opening/closing them are different. The same PBP displays the same direction with different conformations, i.e. the galactose/glucose BP with bound different ligands (galactose, glucose and GGal). It has been proposed that a "balancing interface" serves to stabilize some PBPs in a single open conformation (Davidson *et al.*, 2008; Shilton, 2008).

### 2.1.5  Interactions between protein and ligand complexes

Although there is a diverse range of ligands for known PBPs, (e.g. monosaccharides and disaccharides, amino acids, dianions, etc.) there are some common elements in how each is recognized by its own specific receptor. Hydrogen bonds provide the majority of interactions between the ligand and protein, and are also important for determining the ligand specificity; in essence, for each group of a given ligand that can form hydrogen bonds, protein groups are correctly placed to provide them. These interactions are capable of associate with the ligand and keeping it bound tightly to the binding pocket and able to dissociate by overcoming the low energy barrier while ligand translocation. Van der Waals' interactions strengthen the binding further. For sugar binding proteins, aromatic residues located in the ligand–binding pocket are also a very common feature, providing aromatic stacking and hydrophobic interactions.

### 2.1.6  Proposed model for ligand delivery

The ligand delivery process presumably starts by binding the ligand to one domain of the PBP. It is expected that the ligand preferentially binds to the domain that provides it with more interactions. In the next step the other domain starts moving closer to the ligand by rotating and bending motions at the hinge region. When closure is complete, the ligand is completely trapped in the binding pocket. It is then entirely separated form the bulk solvent, having replaced the water molecules that had interacted with polar residues before ligand binding/closure.

Only the ligand bound closed form can interact productively with the membrane-integral component. To accomplish this, the PBP must have a specific set of residues in both lobes that allow it to interact with the complementary regions of the permease (Sack *et al.*, 1989; Quiocho, 1990).

The PBPs interaction with the membrane integral protein is an active process in which ATP hydrolysis and energy coupling propagation take place. The ligand is thus released from the PBP, and transferred to the cytoplasm through the membrane protein. After unloading its cargo, the permease/PBP complex can then dissociate, allowing a new cycle to begin.

### 2.1.7 Release of PBPs and removing bound ligands (general considerations)

Proteins of the periplasmic space in Gram-negative bacteria can be released using a variety of shock methods. This can be done by making spheroplasts by lysozyme-EDTA treatment, by increasing the osmotic strength by treating cells with highly concentrated sucrose followed by resuspension of the cells in cold water, by cyclic freezing and thawing methods, or by a chloroform shock method. How chloroform release only PBPs is not known. However, PBPs are resistant to chloroform giving the possibility to avoid several centrifugation steps performed in the other shock methods, which is beneficial in protein purification (Ames *et al.*, 1984).

Since PBPs have high affinity to their respective ligands, and in particular, generally have a very low off-rate for the ligand-binding equilibrium (Miller *et al.*, 1980), even over-expressed, highly-purified protein very frequently contains a bound ligand (Miller *et al.*, 1980). For binding and/or structural studies, this bound ligand usually has to be removed. Because the proteins are generally very stable, and easily refolded, reversible denaturation with guanidine-HCl (Miller *et al.*, 1983) or urea is used, followed by exhaustive dialysis.

## 2.2  An overview: conifers defense against root and butt rot disease

### 2.2.1 Responsible agents

Conifers are the most abundant and economically important plant group in the Northern Hemisphere. Timber production is one of the largest industries in Europe, a huge component of the Swedish economy. Like all plants, conifers must survive in a diverse environment that is rich in microorganisms, and so they are susceptible to pathogenic attack. The root and butt rot disease caused by *Heterobasidion* spp. of family Bondarzewiaceae has become a severe problem in temperate forests of the Northern Hemisphere (Asiegbu *et al.*, 2005). It is estimated that losses in the US alone amount to one billion dollars each year.

The fungi belonging to *H. annosum* share the same ecology and morphology. However, mating experiments have shown the existence of at least three intersterile groups/types in Europe, i.e. P, S and F (Korhonen *et al.*, 1992). These groups show host specificity, although some intersterile groups have the capability to attack common conifers and other broad leaved trees grown in mixed groupings with pines (Korhonen *et al.*, 1992). The P, S and F-types attack primarily Scots pine (*Pinus sylvestris* L), Norway spruce (*Picea abies*), and silver fir (*Abies alba*), respectively. Since these fungi degrade both cellulose and lignin components of wood, they are referred as white rot fungi. This ability contributes to their action as a strong parasite and a saprophyte that is able to infect and destroy living conifer roots and stems of all ages as well as dead trees (Fig. 2) (Asiegbu *et al.*, 2005).
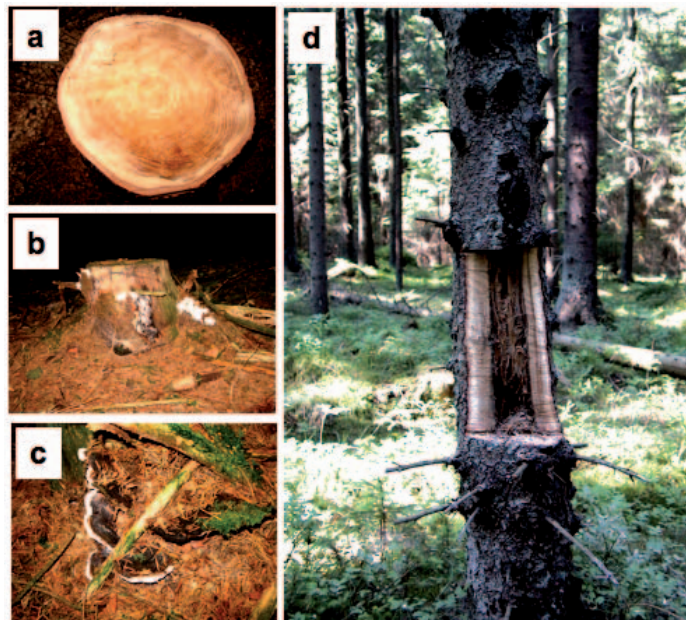


*Figure 2.* (a) Discoloration and decay of a tree infected with *H. annosum*. (b) Base of a *P. sylvestris* trunk attacked by *H. annosum*. Basidiocarps are growing at the base. (c) The fruiting bodies of *H. annosum*. (d) Destruction caused by *H. annosum* to a young Scots pine tree (courtesy of Mattias Berglund and Magnus Pettersson, Southern Swedish Forest Research Centre, SLU).

## 2.2.2 Disease transmission and management

Widespread infection of root and butt rot disease caused by *H. annosum* takes place with high incidence after thinning, in freshly cut stumps.

Wounded and juvenile roots of seedlings also can be infected by airborne basideospores (Asiegbu *et al.*, 1994). The spore adhesion is significant in the mucilaginous regions of the root and butt, but not in the non-slimy regions (Asiegbu, 2000). Root-to-root contact *via* mycelia also spreads the disease by vegetative growth. Abiotic factors such as soil type, nutrients, high pH, and stress conditions further influence disease spread (Piri, 1998).

When the trees are infected by spores, infectious structures become visible within 24 h (Asiegbu *et al.*, 2005). Appressorium formation, penetration and signaling within the host take place in the early infection stage. After 72 h, the late infection stage is expressed by disarranging of the host defense and degrading of tissues (Karlsson *et al.*, 2003). Natural openings and beetle galleries act as frequent routes for infection. The biology of the host-pathogen interaction and disease spreading has been studied extensively, but the molecular mechanisms between the plant and the pathogen have yet to be revealed.

### 2.2.3 Defense mechanism and pathogenic related (PR) proteins

During evolution, plants have developed defense mechanisms against pathogens to minimize their destruction. These defensive measures range from alteration of physical properties, such as the formation of hard bark, waxes on the surface and hard seed coats (Linthorst, 1991), to biochemical defenses. Expression of pathogenesis related (PR) proteins provide a varied array of defense mechanisms. PRs have been defined as proteins encoded by the host plant but induced only by abiotic stress factors such as wounding, UV-radiation, osmotic shock, low temperature, water deficit and excess, as well as biotic stresses from various infectious agents/pathogens, insects, nematodes and herbivores (Antoniw *et al.*, 1980; van Loon *et al.*, 1994). Since many PR proteins act against pathogenic microbes, they often are referred to as antimicrobial proteins or peptides. Some of the development-specific expression patterns of the PR proteins have been recorded during seed germination, embryogenesis, flowering and senescence (Edreva, 2005). PR proteins are distinguished by their biochemical properties such as low molecular weight, stability at low pH or temperature, and high resistance to protease degradation (van Loon & van Strien, 1999).

Five main groups of PR proteins from tobacco were originally characterized using both biochemical and molecular biological techniques (Bol *et al.*, 1990; Broekaert *et al.*, 1997). The classification was based on the amino acid sequence identity, as well as similarity of the enzymatic and biological activities. The list was expanded to 11 PR proteins further (Table 1). The families PR-8 and PR-10 has been found in cucumber and parsley

(van Loon *et al.*, 1994). Later the list was expanded to 14 PR families (PR-1 to PR-14), as three more novel families (PR-12, PR-13 and PR-14) were recognized in radish, *Arabidopsis* and barley, respectively (van Loon, 1999; van Loon & van Strien, 1999). Here, I present a longer list that includes the novel PR family (PR- 17) from *Macadamia integrifoila* (MiAMP1) and *Pinus sylvestris*, which have 64%, sequence identity that we have explored in some detail (Table 1). The NMR structure of the MiAMP1 is available, but nothing was known about such proteins mode of action.

*Table 1.* Proposed PR Families (van Loon & van Strien, 1999; Edreva, 2005), ⋆⋆ indicate the novel PR family identified from this study.

| Family | Properties | Type member |
|---|---|---|
| PR-1 | unknown | Tobacco PR1-a |
| PR-2 | β-1,3 glucanse | Tobacco PR2 |
| PR-3 | chitinase type I, II, IV, V, VI, VII | Tobacco P, Q |
| PR-4 | chitinase type I, II (chitin binding) | Tobacco "R" |
| PR-5 | "thaumatin-like" | Tobacco S |
| PR-6 | proteinase-inhibitor | Tomato inhibitor I |
| PR-7 | endoproteinase | Tomato $P_{6g}$ |
| PR-8 | chitinase type III | Cucumber chitinase |
| PR-9 | peroxidase | Tobacco "lignin-forming peroxidase" |
| PR-10 | "ribonuclease-like" | Parsley "PR1" |
| PR-11 | chitinase type I | Tobacco class V chitinase |
| PR-12 | defensin | Radish Rs-AFP3 |
| PR-13 | thionin | *Arabidopsis* THI2.1 |
| PR-14 | lipid-transfer protein | Barley LTP4 |
| PR-15 | germins | Barley |
| PR-16 | "germins-like" | Pepper |
| PR-17⋆⋆ | β-1,3 glucan binding protein | Scots pine |

PR-1 is the most dominant and abundant among the known families. The antifungal and antibacterial activities of these proteins have been demonstrated, but the exact mode of action is still unknown (van Loon & van Strien, 1999; Edreva, 2005). Enzymatic activities of PR proteins were found for PR-2 and PR-3, which act on glucan and chitin in fungal cell walls (Legrand *et al.*, 1987). Chitinase activity has further been detected for PR-4, PR-8 and PR-11. PR-4 consists of chitin binding domains. PR-6, PR-7, PR-9 and PR-10 are established to have proteinase, peroxidase, ribonuclease and lysozyme activities. PR-15 and 16 designated to germins

and "germin-like" proteins constitute a large and highly diverse family of ubiquitous proteins (Bernier & Berna, 2001; Park *et al.*, 2004). Sp-AMP3 and MiAMP1 are not similar to any known PR protein, and so this group of PR proteins can be categorized as PR-17.

The antifungal activity is one of the most important common features of the known PR protein families. Hydrolytic enzymes such as $\beta$-1,3 glucanases, chitinases and proteinases are capable of degrading the fungal cell wall, which is a mixture of glucans, chitins and other proteins. Thaumatin, defensin, thionin and lipid transferase proteins are able to destroy the fungal cell wall, so inhibiting growth (van Loon & van Strien, 1999). Despite the obvious diversity, there is a strong link between the action of many antimicrobial proteins and some form of action or interaction with common sugars of the fungal cell wall.

In plants, after localized exposure to pathogens or hypersensitive responses, the systemic acquired resistance (SAR) pathway is activated (Ryals *et al.*, 1996). SAR is analogous to the innate immune system found in animals, which plays an important role in resisting pathogens prior to infection. The SAR system is tightly correlated with PR proteins, i.e. those expressed in response to pathogenic attacks. PR proteins are recognized as markers for the SAR system, and PR genes are recognized in the SAR gene list.

Even though many antifungal proteins are known, the molecular mechanism involved in most cases is yet to be revealed.

# 3    Discussion

## 3.1    Paper I: Glucose/galactose binding protein

### 3.1.1    GGal: another natural ligand transported *via* MeGal

This section describes the structure of glucose/galactose binding protein (GBP) from *Salmonella typhimurium*, in complex with 2R-glyceryl-β-D-galactopyranoside (hereafter referred as GGal), one of its physiological ligands. GBP was the first PBP described, in terms of its ability to transport glucose and galactose and its roles in chemoreception (Boos, 1972).

GGal is one of the most abundant natural glycolipids found in plants. Some plants have up to 20% of GGal in terms of their total lipids (Weenink, 1961; Sastry & Kates, 1964). GGal is derived from breakdown of the lipids of animal cells, and Enterobacteriaceae, found in animal guts, encounter this substrate in large quantities. To transport galactose, six active transport systems are actively engaged in *E. coli* (Rotman *et al.*, 1968; Kalckar, 1971). Only two of them, the β-methylgalactoside transport system (MeGal) and the lactose transport system can transport GGal (Wilson, 1974). This compound is also known to be a substrate for the enzyme β-galactosidase and an inducer for expression from the lactose (lac) operon (Burstein *et al.*, 1965). Even though *Salmonella* has a deletion of the entire lac operon, GGal still can be transported *via* MeGal system in *Salmonella*, and the metabolism is expected to be accomplished by some other β-galactosidase(s) pathway. The $K_m$ and $K_D$ values for GGal recorded as remarkably low, close to the values of glucose and galactose (Anraku, 1968; Boos, 1969).

When the GGal enters to the cell, β-galactosidase breaks it down to form glycerol and galactose. Other enzymes then can convert this into glycerol-3-phosphate, and then dihydroxyacetone phosphate and glyceraldyhyde-3-

phosphate, which enter into glycolysis. Phosphorylated galactose is converted to UDP-galactose by the action of a transferase. Epimerase acts on UDP-galactose and produce UDP-glucose, which is a raw material for glycolysis (Fig. 3).
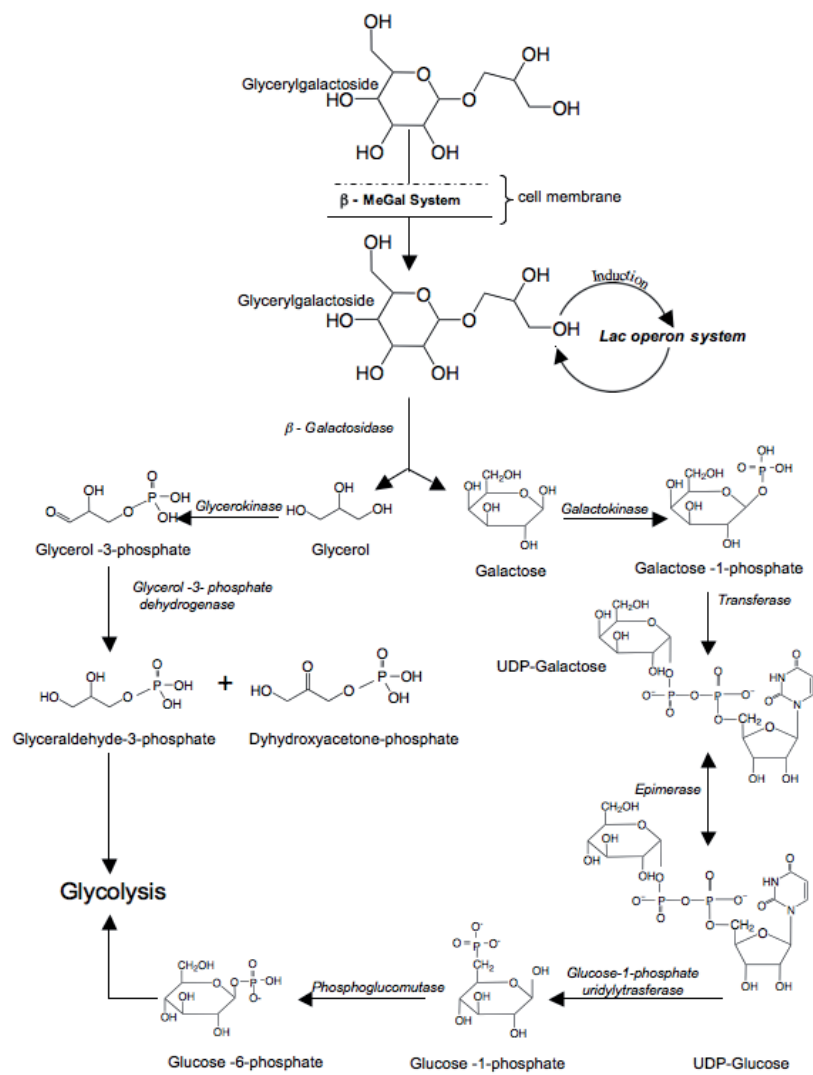


*Figure 3.* Fate of GGal inside the cell.

### 3.1.2 Protein purification, crystallization and structure determination

Protein expression made use of an existing plasmid, and purification followed an osmotic shock procedure to extract periplasmic binding proteins, as described in Paper 1. Initial crystallization trials were carried out using commercially available screening kits. For the structural work described here, the protein was crystallized under the following conditions: equal volumes of the reservoir solution (20% polyethyleneglycol (PEG) 3350, 0.2 M NaSCN) and protein solution (composed of 0.29 mM (10 mg/ml) protein and 0.60 mM GGal, synthesized as described earlier by W. Boos (Boos, 1982)) were mixed and equilibrated against the reservoir solution by vapor diffusion at room temperature. Streak seeding was done immediately after setting up the drops. Thin plate-like crystals appeared after 24 h (Fig. 4).
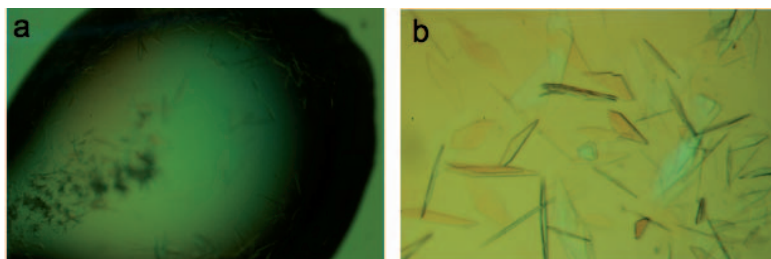


*Figure 4.* GBP crystals (a) Needle-like small crystals from the initial crystallization trials used for seeding, to obtain. (b) optimized crystals.

Crystals were stabilized by transferring to a cryoprotectant containing mother liquor with an increased PEG 3350 concentration (up to 30%), and flash-cooled directly in liquid nitrogen.

The structures of GBP from *E. coli* and *Salmonella* were available with and without ligands (Mowbray & Petsko, 1983; Vyas *et al.*, 1983; Mowbray *et al.*, 1990; Zou *et al.*, 1993). The structure was solved by molecular replacement with MOLREP (Vagin & Teplyakov, 1997), using the unliganded GBP structure as search model, PDB entry code 1GCG (Zou *et al.*, 1993). The structure was then improved with rigid-body and restrained refinement in REFMAC5 (Murshudov *et al.*, 1997). Statistics for data collection and refinement are shown in the Table I of Paper 1.

### 3.1.3 Overall structure

The final structure of the GBP/GGal complex consists of two molecules in the asymmetric unit, each having two similar globular domains. The two domains are connected to each other by a three-stranded hinge region. Both

domains represent a β-sheet, sandwiched between two layers of α helices (Fig. 5a). Structural sodium and calcium ions were observed in each molecule, in the loops following the first helixes in N terminal domain and C terminal domain (Fig. 5a). Though the bound $Ca^{+2}$ was reported before (Vyas *et al.*, 1987), this is the first time a sodium ion reported. The electron density found between two molecules is thought to represent a thiocyanate ion, which comes from the mother liquor (including NaSCN); this ion is not thought to be structurally important.
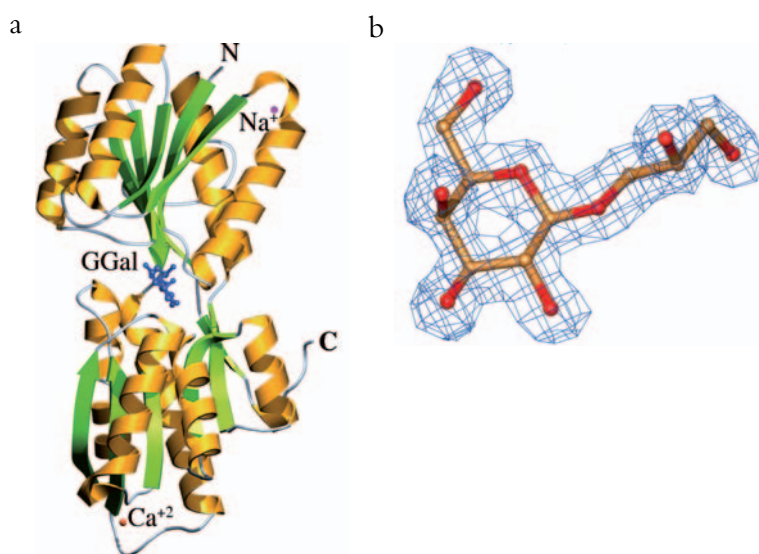


*Figure 5.* (a) The overall structure of the GGal bound GBP. (b) Electron density of the GGal in the SIGMAA-weighted ($2F_o$-$F_c$) map (Read, 1986) contoured at 1 σ=0.49 e/Å$^3$.

### 3.1.4 Ligand binding

The binding of the ligand was confirmed by very clear electron density in the ligand-binding pocket (Fig. 5b). The hydrogen-bonding network consists of residues from both domains, 6 from N terminal domain and 9 from C terminal domain. In addition to the previously reported hydrogen bonds for glucose and galactose complexes, residues Thr110, Asp154 and Gln261 interact with the glycerol moiety. As well as making hydrogen bonds with the –CH$_2$OH group, Asn91 interacts with O2′ of the glyceryl moiety. Asn256 interacts with the glycoside oxygen of the GGal, i.e. O1.

Two water molecules are involved in the hydrogen-bonding network, one of them interacting solely with the glyceryl moiety (Fig. 6a).

The binding pattern was analyzed for similar GBP sequences, and the residues involving in binding the sugar unit were seen to be conserved. The residues that interact with the glyceryl moiety are also conserved or replaced by a residue that is expected to act similarly. This suggests that GBP's role in binding and transporting GGal is widespread in nature.
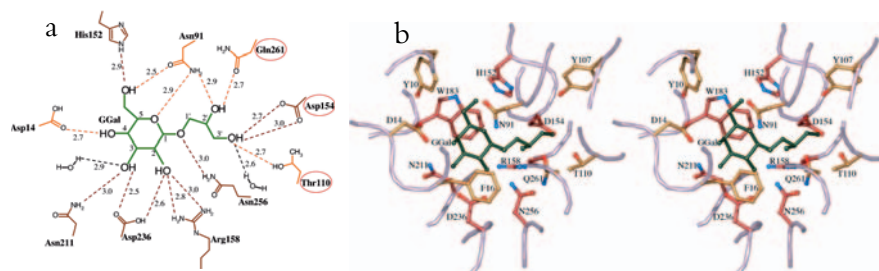


*Figure 6.* The ligand-binding pocket. Panel (a) shows the hydrogen-bonding network between GGal and GBP. Panel (b) shows the interactions in the binding site residues including residues that make stacking interactions with the GGal.

### 3.1.5 "Fan" of related conformations

Superposition of the available GBP structures, including the structures from *E. coli* and *Salmonella* (PDB entries 3GA5, 2GBP, 1GLG, 2HPH, 2IPN, 2IPM, 2IPL, 1GCA, 3GBP, 1GCG, 2FVY, 2FWO), (Flocco & Mowbray, 1994; Vyas *et al.*, 1994; Borrok *et al.*, 2007) with and without ligands, reveals just how the ligand binding is associated with conformational changes. The two molecules in the same asymmetric unit of the GGal complex structure showed ∼1.5° difference in terms of the relationships between the two domains. *Salmonella* GBP structures in complex with glucose (3GBP) and galactose (1GCA) both are slightly more open than the GGal complex. This is probably due to the extra hydrogen bonds compared to the glucose and galactose bound complexes. 2FWO, the open–apo GBP structure demonstrates the most open form (∼37°). The superimposed structures illustrate the "fan"-like spread of conformational changes seen, from the most open structure to the most closed structure, consistent with a single preferred conformational pathways for its motions (Fig. 7).
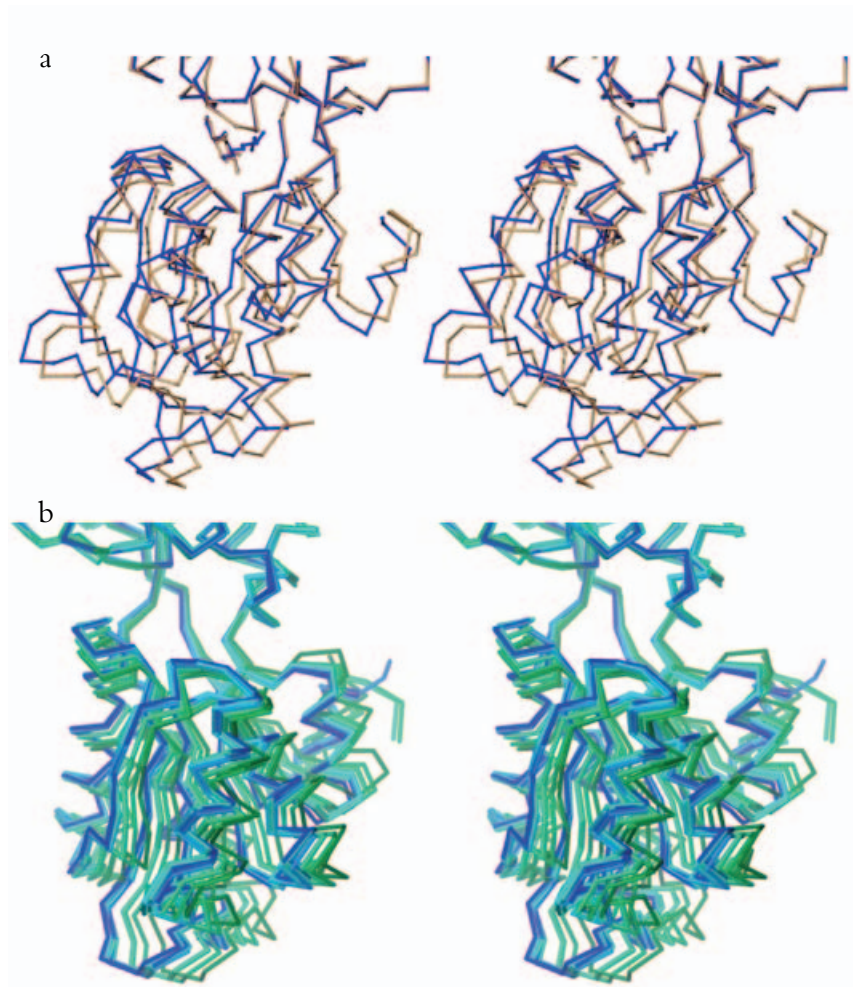
*Figure* 7. Conformational changes of GBP structures. Panel (a) shows a stereo view of the superimposed structures of the complex with bound galactose (PDB entry 1GCA, gray) on the GGal complex (PDB entry 3GA5, dark-gray). Panel (b) shows conformational changes of available GBP structures from *E. coli* and *Salmonella*. The Domain 1 is superimposed. Dark-gray color represents the closest GGal complex and the gray color represents other available complexes. In the series, GGal, GGal molecule B (1.5°), 2GBP (1.7°), 1GLG (1.8°), 2IPN (2.0°), 2HPH (2.0°), 2IPM (2.0°), 2IPL (3.4°), 1GCA (5.1°), 3GBP (5.4°), 1GCG (7.0°), 2FVY (9.8°). For simplicity, the most open 2FWO (36.8°) was not shown.

## 3.2   Paper II: Xylose binding protein

### 3.2.1  The aim of the study

Both Gram–negative bacteria, e.g. *E. coli* and *Salmonella* (Lin, 1987), and Gram–positive bacteria, e.g. *Lactobassilus protosus* MD353, (Lokman *et al.*, 1994), can utilize D-xylose as their sole carbon source. The sugar is transported either *via* a binding protein depending ABC transport system or through a low affinity transport system. In the low affinity system, XylE encodes the proton symporter, which is a single membrane protein that operates using a gradient of protons as the energy source (Lam *et al.*, 1980). *xylFGH* genes encodes the ABC type transporters (Song & Park, 1997). The three components, the periplasmic xylose-binding protein (XBP), the ATP binding unit and the membrane permease are encoded as XylF, XylG and XylH, respectively.
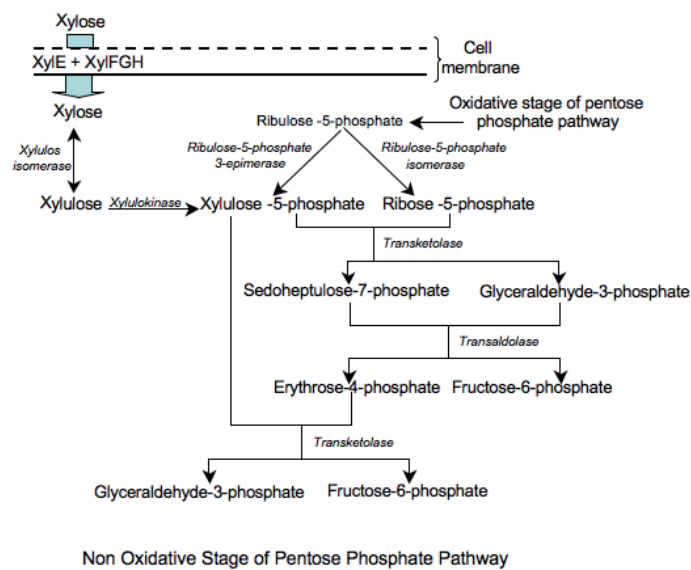


*Figure 8.* Dissemination of D–xylose

31

Metabolism of D-xylose occurs through the pentose phosphate pathway with the help of the enzymes xylose isomerase and xylulokinase, which are encoded by the genes *xylA* and *xylB* (David & Wiesmeyer, 1970; Song & Park, 1997). Once it has entered into the cell, the sugar is first isomerized to xylulose by the isomerase, and then phosphorylated to give xylulose-5-phosphate by the xylulokinase. Xylulose-5-phosphate then enters into the non–oxidative stage of the pentose phosphate pathway (Fig. 8).

The aim of this study is determine the X–ray crystal structures of different conformations of the XBP, when binding the relevant ligand.

### 3.2.2 Cloning, protein expression, purification and crystallization

Cloning, expression and purification of the protein has been done as described in the methods section of Paper II. The purified protein samples were denatured and then refolded using exhaustive dialysis in order to remove endogenously bound ligands.
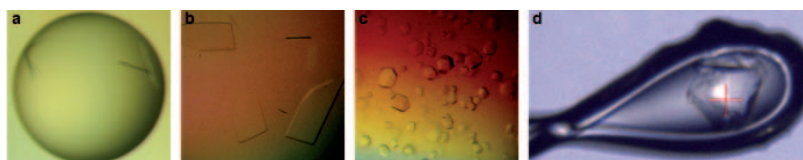


*Figure 9*. XBP crystals. (a) Initial crystal screening hit for ligand free XBP used for seeding. (b) Crystals from optimized conditions. (c) Hexagonal shaped crystals obtained after co-crystallization of XBP with xylose. (d) XBP crystal mounted in a loop before data collection.

Crystallization screening trials were done using the hanging drop vapor diffusion method. XBP ligand free protein sample was crystallized (Fig. 9) in the presence of 21% w/v PEG 3350, 0.2 M ammonium dihydrogen phosphate at pH 7.5. Soon after setting up, the crystallization drops were streak seeded. Soaking of the crystals with 1.3 mM xylose in mother liquor with an increased PEG 3350 concentration (up to 35%) resulted in the open liganded form (XBP-cls-xyl) of the structure. Co-crystallization of 0.5 mM XBP with 1.5 mM D-xylose generated the closed-liganded (XBP-cls-xyl) structure of XBP. These crystals were grown in 2.4 M sodium malonate at pH 7.0, and were flash cooled directly in liquid nitrogen without a cryoprotectant.

### 3.2.3 Overall structures

The X-ray structures of XBP show that, like GBP, its architecture agrees with the previously described pentose and hexose sugar binding proteins. All three XBP structures display the typical fold for hexose/pentose sugars, with two similar globular domains connected by three stranded hinge region. The ligand binding takes place in the domain interface (Fig. 10).
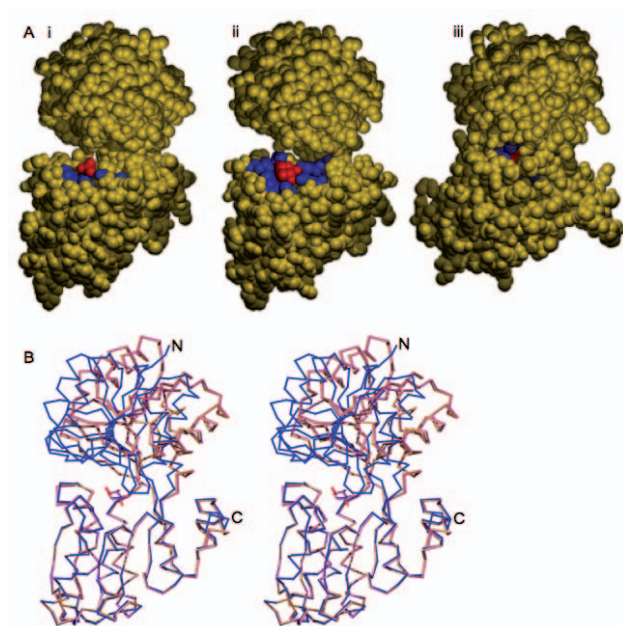


*Figure 10*. Space-filling models of XBP structures. Panel (A) i. Open apo structure of XBP. The bound phosphate ion in the binding pocket and corresponding binding residues from C–terminal domain are shown in red and blue. ii & iii. Open and closed xylose bound XBP structures. The bound xylose molecule to the C-terminal domain and corresponding binding residues are shown in red and blue, respectively. Panel (B) Conformational changes of XBP. Stereo representation of the superimposed Cα backbone of the C–terminal domains of the open ligand free, open liganded and closed liganded XBP structures are in gold, golden-red and blue.

The ligand free open structure was solved by the molecular replacement method using MOLREP (Vagin & Teplyakov, 1997), with the *Thermoanaerobacter tengcongensis* ribose binding protein (TtRBP, PDB entry code 2IOY (Cuneo *et al.*, 2008b), and refined to 2.1 Å resolution using REFMAC5 (Murshudov *et al.*, 1997) as described in detail in Paper II. The ligand free open structure was used as the starting model for the XBP-opn-xyl structure. The closed liganded XBP structure was solved using the intact

TtRBP, which is also a closed form. The statistics for data collection and refinement are shown in Table 1 of Paper II.

### 3.2.4 Ligand binding

In both XBP-opn–xyl and XBP-cls-xyl structures, the sugar displays the β-anomeric form. Binding of the α-anomer would disturb the bonding interactions that O1 makes with Asp135 and Asn137. The electron density maps showed only the presence of the β-anomer of xylose in these XBP structures, although the presence of 25% of the α-anomer cannot be ruled out on the basis of electron density alone.

In both xylose bound structures, D-xylose appeared as the most stable chair-conformer pyranose (6-membered ring) form that dominates in solution (Reeves, 1951). Since the five carbon sugar lacks a $-CH_2OH$ group protruding from the pyranose ring, the β-anomeric sugar displays a symmetrical arrangement of its −OH groups (Figs. 11 and 13) and can in theory be fitted into the electron density in two possible ways. The correct orientation of the sugar was ultimately decided by listing the possible hydrogen bonds in both orientations, and taking the interactions with the sugar ring oxygen into an account (Fig 11). In the XBP-opn–xyl structure, both sugar orientations show seven hydrogen bonds but none with the ring oxygen. Both ways, three water molecules are bonding with O1, O2 and O3. However, only one of the orientations of the sugar in the XBP-cls-xyl structure placed the ring oxygen in a position to make a hydrogen bond; this was taken as the correct sugar orientation. We therefore, believe this to be the favored orientation, but cannot rule out the possibility that the other mode of binding occurs with lower frequency.

Residues Asp135, Asn137, Asn196, Asp222 and Lys242 from the C-terminal domain of the XBP-opn–xyl structure interact with the β-anomeric form of the sugar. As stated above, three water molecules form hydrogen bonds with O1, O2 and O3. Phe141 and Trp169 further support the ligand binding by hydrophobic interactions.

In the XBP-cls-xyl structure, the hydrogen–bonding network consists of 12 hydrogen bonds, five from the N-terminal domain, and seven from the C-terminal domain. The ring oxygen of the sugar molecule now interacts with Arg91 (Fig.11d). Other than this Arg16, Asp90 and Arg91 from the N-terminal domain make hydrogen bonds with O1, O2, O3, replacing three water molecules in the open structure. The interaction distances also get shorter and stronger (Figs. 11 and 12) in the closed structure.
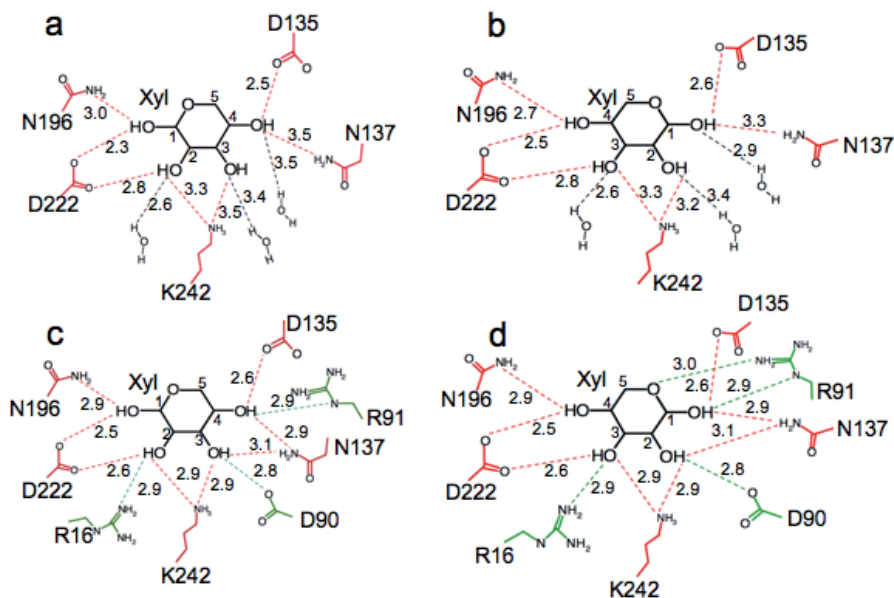
*Figure 11.* Determining the orientation of bound xylose. The ligand–binding pocket shows the arrangement of binding of the ligand in both possible orientations of the D-xylose molecule. Panels (a) and (b) show the ligand bound open form. Panels (c) and (d) show the possible orientations of the sugar molecule in the closed ligand bounded structure. N- and C-terminal residues are marked in green and red, respectively.
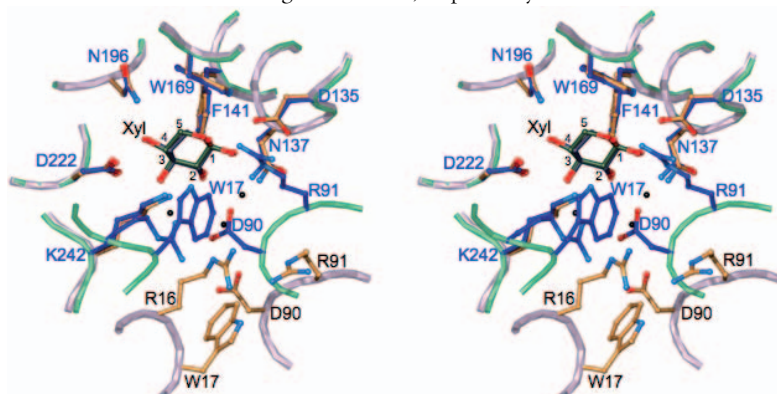


*Figure 12.* Stereo representation of superimposed binding site residues of XBP open and closed structures. The residues in gold color represent the XBP-opn–xyl structure, and the blue color represents the residues in the closed structure. The thistle and green colors of the rattles are for the open and closed structures, respectively.

### 3.2.5 Other possible ligands

Other than xylose, ribose, which is its C3 epimer (Fig. 13b), is expected to be transported by XBP (Song & Park, 1998). Assuming the same mode of binding, D–ribose would have three less hydrogen bonds than D–xylose (Fig. 14a).
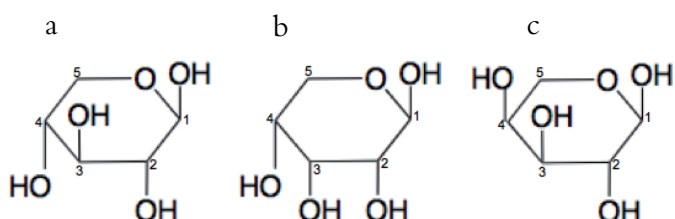


*Figure 13.* The possible ligands for XBP. Panels (a), (b) and (c) display β-D-xylose, β-D-ribose and β-L-arabinose, respectively.
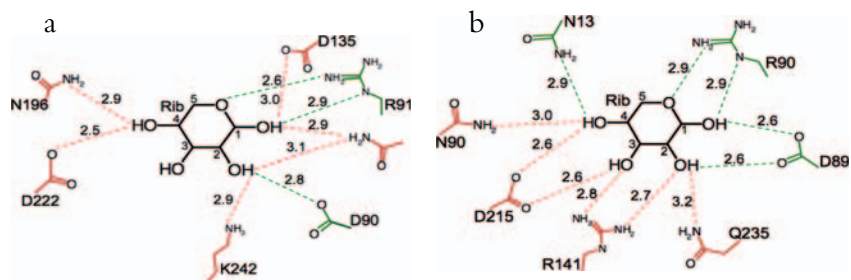


*Figure 14.* Ribose binding in XBP and in RBP. Panel (a) shows D-ribose docked in the XBP closed structure. Panel (b) shows D-ribose as it bound in RBP (PDB entry 2DRI).

Compared to ribose binding to its own binding protein, RBP (PDB entry 2DRI), this is also two less hydrogen bonds (Fig. 14b). L-arabinose, which is sterically similar to D–xylose in terms of the second, third, and fifth hydroxyl groups (i.e. it is the C4–epimer of xylose, Fig. 13c) is also another possible ligand which can be transported *via* XBP (Shamanna & Sanderson, 1979), however, this ligand would also make fewer hydrogen bonds than xylose.

The steric similarities of these sugars (Fig. 13) allow them to bind and transport trough the system. The fluorescence measurements of the three sugars confirm this argument further. The $K_D$ value of D–xylose measured in this study (0.13 μM at 25 °C) agrees with the previous estimations of the sugar binding (Ahlem *et al.*, 1982). Ribose showed an ~50 times higher $K_D$ value that xylose, whereas L–arabinose had ~100-fold weaker binding.

We conclude that D-xylose is the most preferred ligand for XBP but that D-ribose and L-arabinose can act as secondary or backup ligands. These secondary sugars would not compete effectively with xylose, but in a xylose-free environment, would be possible natural ligands for the entire transport system.

### 3.2.6 Conformational changes

The study reveals the different conformations of the XBP that are linked to ligand binding. This is the first time that structures of unliganded open, liganded open and liganded closed forms of one individual periplasmic binding protein are presented together. The open liganded structure that is presented here is the first one of the hexose/pentose sugar-binding cluster, and the only high-resolution one to date.

Ligand associated conformational changes of XBP, like those of most PBPs, are mostly concentrated in the hinge region (Fig. 15a), which play a role in clamping the ligand in between the two domains. Changes at the same points in the hinge segments would lead to greater or lesser degrees of opening around axes that pass near residue 104, and between residues 242 and 243 (Fig. 15b). It is indeed not vital that there is a unique open conformation, merely that the open and closed conformations must be distinct, if they are to function correctly within the ABC transport system. Based on studies of RBP and ALBP (Magnusson *et al.*, 2002), we expect that the open form observed here is not the only one possible, but instead is one member of a family of related conformations in solution.

In three XBP structures, unliganded open, liganded open and liganded closed, Asp90, Asp222, Thr295 are conserved Ramachandran outliers. Both Asp90 and Asp222 act as ligand interactive residues. These two residues are shown as outliers and locate in the same place in the whole cluster of pentos/hexose binding proteins. In GBP Asp90 is replaced by Asn91 and in ABP Asp 222 replaced by Asn221.

The sequence comparisons (Fig. 5 in paper II) were carried out for XBP and the other related sequences including RBP, GBP, ALBP, ABP and other related proteins from the BLAST search. In the XBP sequences all the residues that interact with the ligand are highly conserved. Even though the sequence identity is only 58% in *T. tengcongensis* (2IOY, (Cuneo *et al.*, 2008b)) and *E.coli* RBP structures (Bjorkman *et al.*, 1994; Bjorkman & Mowbray, 1998) the ligand interactive residues are 100% conserved. Compared to the XBP, most of these residues are conserved or replaced by a residue, which can help for the mechanism e.g. Phe for Trp in RBP structures.
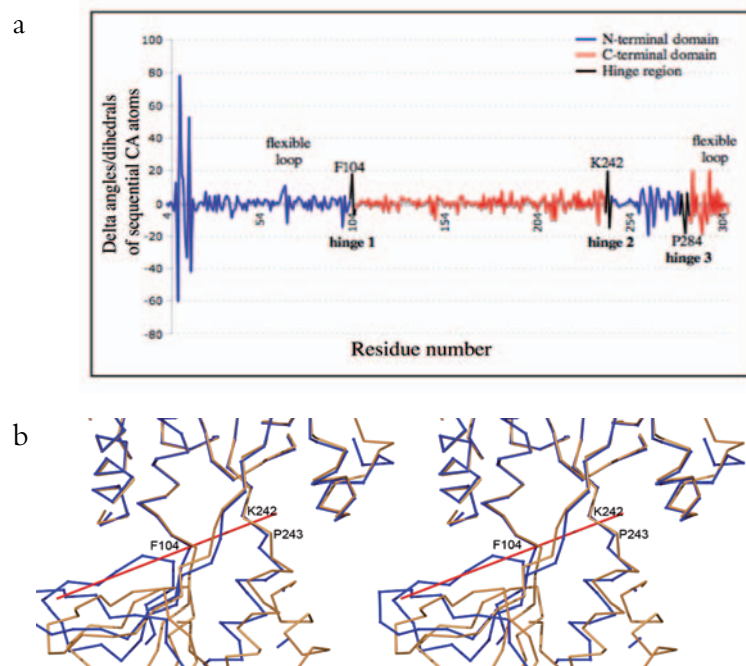
*Figure 15.* Differences in the main chain conformation. (a) Cα ± torsion angle difference were calculated using DDihe (delta-dihedral plots for backbone comparison, (Kleywegt & Jones, 1997)) plot for the whole molecule. (b) Open and closed forms of XBP (gray/dark-gray), are aligned using the C-terminal domain. Rotation axes for opening/closing are shown in gray color.

As for other binding proteins, it is assumed that opening and closing at the hinge occurs continuously in solution, with the open form being favored in the absence of ligand. The open liganded structure can be viewed as an intermediate stage between the open and closed forms in the transport process. Since all the protein–sugar interactions are concentrated in the C-terminal domain (Fig. 11b), this must be the initial binding site. In the next step, the hinge bending motions bring both domains closer extending the ligand binding interactions to the other domain. The closure of the structure would keep the ligand unassociated from the solvent bulk (Fig. 11d). This diminishes the hydration energy in the early steps in the active transportation, but there are no proofs yet, whether the rehydration take place after translocation of the substrate to membrane permease.

38

The mechanism of transferring the sugar molecule to the membrane permease is not clearly understood yet but it has been mentioned that the membrane component only can recognize the closed liganded form.

## 3.3  Paper III: Scots pine antimicrobial protein

### 3.3.1  Why AMP is so important?

*Heterobasidion annosum* is the most destructive fungal pathogen in forests of the Northern Hemisphere. The vegetative growth of the fungi, the destruction it causes, and the ways in which the associated root and butt rot disease is spread have been studied intensively. However, the interactions between the pathogen and its conifer hosts, and the molecular mechanisms that underlie them, are still not understood. Such knowledge would give new insights into how one might control the spread of the disease. In this study we tried to understand the mechanism by which a particular antimicrobial peptides secreted by Scots pine (Sp-AMP) protects it against pathogen attack.

The Sp-AMP (1-5) protein family was originally identified from Scots pine, as being encoded by genes that are highly transcribed in infected pine roots (Asigbu, 2005). The isolated genes were highly related. Alignment of the full-length amino acid sequences revealed few differences; Sp-AMP2 and Sp-AMP4 are identical at the amino acid level. The cysteine-rich polypeptide chains are 105 amino acids long; each includes an N-terminal 26-residue region predicted to be a signal sequence. Sp-AMP3, which is the subject of this study, has molecular weight of 8.5 kDa and is highly basic (pI 8.6). The peptide chain has 6 cysteines, thought to be involved in disulfide bonds.

### 3.3.2  Protein expression

Obtaining the protein directly from pine trees is time-consuming and yields are small. The use of *E. coli* as an expression system to obtain recombinant Sp-AMP3 was not successful. Good expression is easily obtained, but only as inclusion bodies, and the refolding trials were extremely unrewarding. A successful protein expression of similar protein from *Macadamia integrifolia* (sequence identity 64%) in yeast was reported elsewhere (McManus *et al.*, 1999), and so we decided to change to the *Pichia pastoris* system. Two constructs, with and without poly His-tags (at the C-terminus), were designed, and protein expression and purification were carried out as

described in Paper III. After growth of 1 L of an induced YP medium culture, the Sp–AMP3 yield was 0.4 mg.

### 3.3.3 Functional analysis of Sp-AMP3

We first tested whether Sp-AMP3 binds insoluble carbohydrates that are common in fungal cell walls. 20 μg of chitin, chitosan and β–(1-3)–D-glucan (curdlan) powder were each separately mixed with 30 μl of 0.75 mg/ml Sp-AMP3 solution and incubated at 4 °C for 6 h. The samples were then centrifuged for 10 min at 16000 x g. The supernatant was removed and the pellet was washed with 1 M NaCl, followed by 10% acetic acid to detach the remaining bound protein.

The SDS-PAGE analysis showed that Sp-AMP3 did not bind to chitin and chitosan (i.e. the protein was in the supernatant), but it did bind to curdlan (i.e. the protein was only detached after treating the pellet with acetic acid), see Figs. 16 and 17.
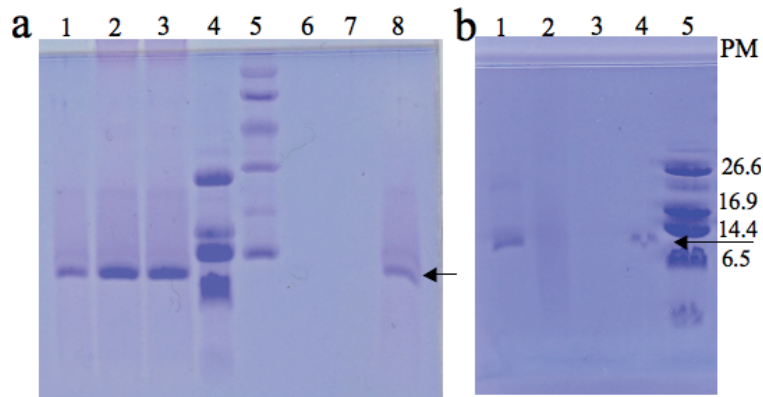


*Figure 16.* (a) SDS-PAGE analysis of the Sp-AMP3 samples after they were incubated with chitin and chitin/chitosan powder. (Starting from left: lane 1, pure Sp-AMP3 sample in 10 mM HEPES, pH 7.0; lane 2, supernatant after incubation with chitin powder; lane 3, supernatant after incubation with chitin/chitosan powder; lane 4, polypeptide marker (PM), the size from top to bottom 26.6, 16.9, 14.4, 6.5, 3.5, 1.4 kDa; lane 5, low molecular weight marker (LMW), the size from top to bottom 94, 67, 43, 30, 21, 14 kDa; lane 6, supernatant after washing the Sp-AMP3-treated chitin sample with 1 M NaCl + 10% acetic acid; lane 7, supernatant after washing the Sp-AMP3-treated chitin/chitosan sample with 1 M NaCl + 10% acetic acid; lane 8, pure Sp-AMP3). (b) SDS-PAGE analysis of the Sp-AMP3 samples after incubation with curdlan. (Starting from left: lane 1, pure Sp-AMP3; lane 2, supernatant after incubation with curdlan; lane 3, supernatant after washing the Sp-AMP3-treated sample with 10 mM HEPES, pH 7.0; lane 4, supernatant after the sample washed with 1 M NaCl + 10% acetic acid; lane 5, LMW). 1.0 μl of the sample was loaded in each lane. The arrow indicates the band expected (9.6 kDa).
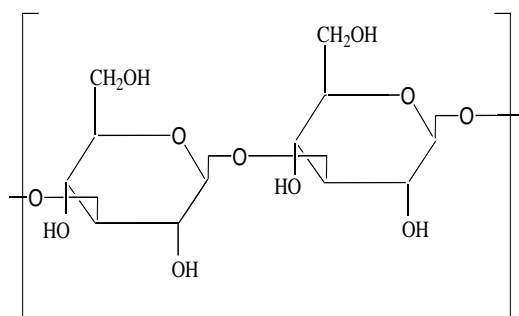
*Figure 17*. Structure of β−1,3 glucan (curdlan).

### 3.3.4 Determination of antifungal activity

Antifungal activity of Sp-AMP3 was studied by observing *H. annosum* (strain FP5) growth on Hagem agar plates (0.5% glucose, 0.05% $NH_4NO_3$, 0.05% $KH_2PO_4$, 0.05% $MgSO_4.7H_2O$, 0.5% malt extract, 2.0% agar, pH 5.5). An agar plug containing *H. annosum* mycelia was placed at the center of a Petri dish containing 20 ml of the medium, and incubated in the dark at room temperature until the mycelia reached a diameter of 1 cm. A sterilized filter paper disc containing 10 μl of 0.75 mg/ml Sp-AMP3 solution was placed at the growth front of the mycelia. The controls were the samples collected before induction of protein expression, and the protein storage buffer (10 mM HEPES, pH 7.0). The plates were incubated in the dark further, and the inhibition observed. The same protocol was followed for the protein both with and without the poly-His tag.

The inhibition of spore germination was investigated after spreading a spore suspension in sterilized water evenly on sterile Hagem agar plates. 10 μl of 0.75 mg/ml Sp-AMP3 solution were added to the sterilized filter paper disks, which were placed on the plates, followed by incubation in the dark, at room temperature for one week. The 10 μl of protein solution was added after every 24 h.

Strong inhibiting activity was seen for both spore germination and hyphal extension, even at the low concentrations of the Sp-AMP3 that could be tested (Fig. 18).
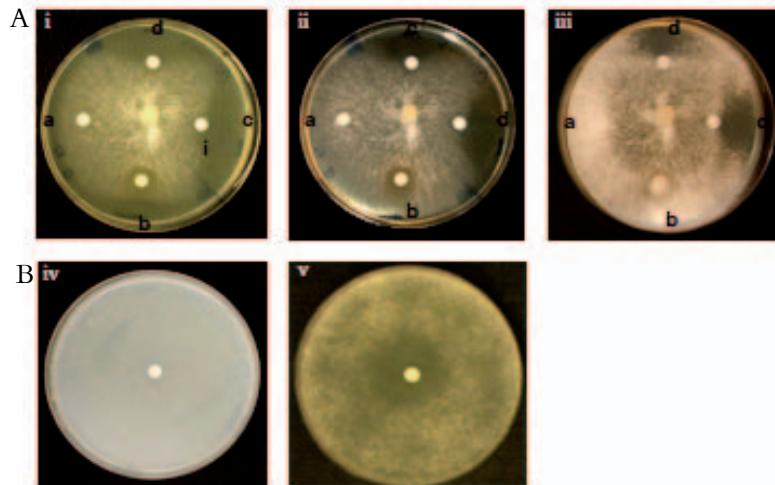
*Figure 18.* Activity screening of Sp-AMP3 against *H. annosum*. (A) Inhibition of vegetative growth. Treatments were started two days after the *H. annosum* inoculation. Sterilized filter paper disks, which were placed on the growing front of the fungal hyphae, were soaked with 10 μl of relevant samples at intervals of 24 h for three days. Pictures i, ii and iii represent the observations after 2, 3 and 5 days of Sp-AMP3 treatment, respectively. (a) 10 mM HEPES. (b) sample taken before the induction. (c) protein sample without His tag, and (d) protein with His tag. (B) Inhibition of spore germination. 100 μl of spore suspension in sterile water was evenly spread on Hagam agar plates and sterile filter paper disks soaked with (iv) 10 mM HEPES, pH 7.0, or (v) 10 μl of 0.75 mg/ml Sp-AMP3 solution in 10 mM HEPES, pH 7.0, were placed in the middle of the plate and incubated at room temperature for hyphal growth for seven days. White zones indicate the growth areas, whereas the cleared zone in plate (v) indicates growth inhibition.

### 3.3.5 Homology Modeling of Sp-AMP3

Sp-AMP3 was modeled using the *Macadamia integrifolia* antimicrobial protein (MiAMP1) NMR structure (PDB entry 1C01, identity 64%) as the template, as described in Paper III.

The homology modeling studies showed that Sp-AMPs are expected to have the Greek key β–barrel fold (Fig. 19a). There is no obvious active site cavity or cleft as in enzymes and therefore, no enzymatic reactions would be expected. There are 3 conserved disulfide bonds and a number of other conserved residues. Some of the conserved residues are clustered on one face of the molecule, forming a surface patch as shown in Fig. 19b. A sequence alignment, showing Sp-AMP3, MiAMP1 and a more distant relative (*Streptomyces* killer toxin–like protein), is presented in Fig. 20.
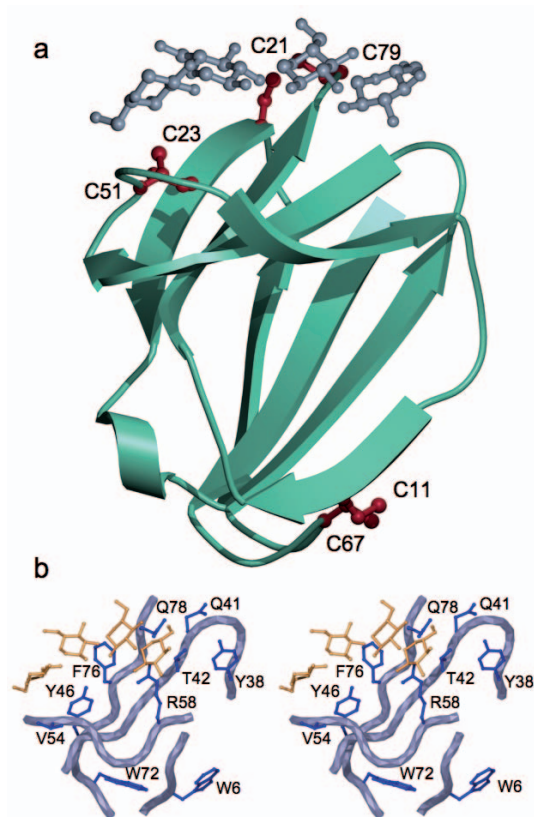
*Figure 19.* Homology model of Sp-AMP3. (a) Sp-AMP3 model showing the disulfide bond forming residues in maroon. (b) Predicted binding site residues with modeled β -(1,3)-D-glucan in gold.



*Figure 20.* Sequence alignment. Related sequences were identified by a DALI search (Holm, 1998). The conserved residues are highlighted in red. The proteins identified represent the NMR structure of MiAMP1, a plant antimicrobial protein (1C01, 76), and *Streptomyces* killer toxin-like protein (1F53, 84).
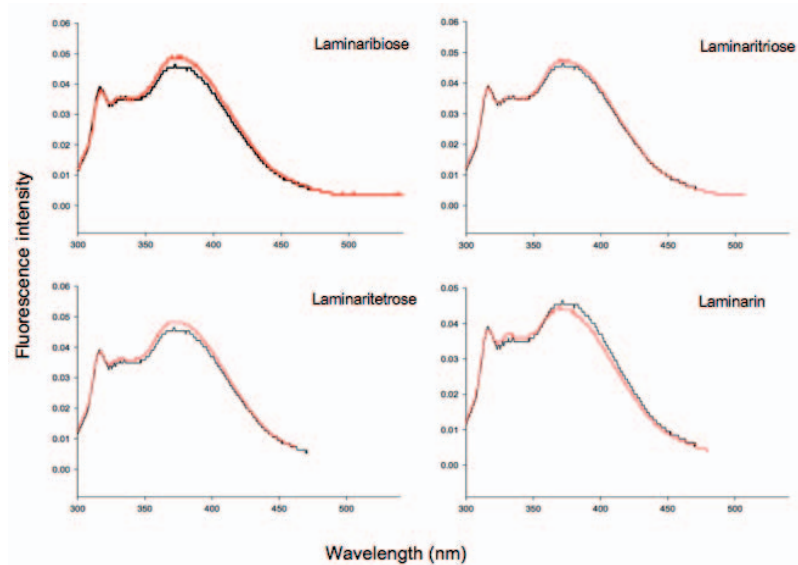
*Figure 21.* Fluorescence spectra of Sp-AMP3. Fluorescence changes were measured in the presence of laminari-oligosaccharides. 0.5 μM of protein in 10 mM HEPES, pH 7.0, was used. The spectra were recorded at 25 °C
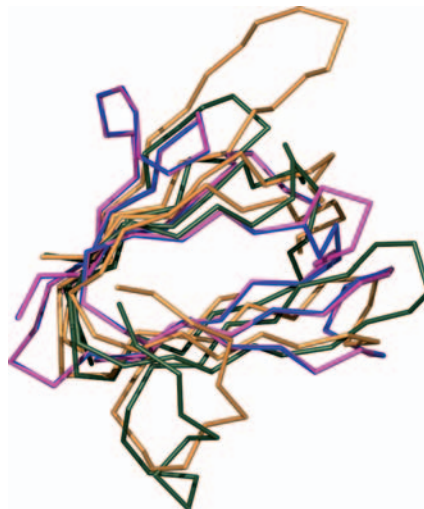


*Figure 22.* Superposition of the Sp-AMP3 homology model on the structures with similar folds. The Sp-AMP3 model is in violet-red, MiAMP1 (PDB entry 1C01) is in blue, antifungal protein from *Streptomyces tendae* TU901 (PDB entry 1G6E) is in gold, and *Streptomyces* killer toxin-like protein (PDB entry 1F53) is in dark-green.

44

### 3.3.6 Fluorescence spectroscopic studies

Fluorescence measurements were carried out as described in Paper III, to investigate the binding of soluble sugars such as β-1,3 glucan sugars up to laminariheptose, laminarin (an undefined soluble polymer with β-1,3 glucan and β-1,6 glucan linkages in an approximately 3:1 ratio), cellobiose, cellotriose, cellopentose and glucose on Sp-AMP3. Excitation and emission wavelengths of 285 nm and 382 nm were used in titrations. The sugars with reasonable changes of the fluorescence intensities are shown in Fig. 21.

There are only two tryptophans in the model, both located outside the proposed binding site. However, the fluorescence results suggested that ligand binding promotes a conformational change in the whole protein that is sensed by the tryptophan residues.

### 3.3.7 A proposed binding site for β-1,3 glucans

As noted above, the homology model of the Sp-AMP3 structure does not suggest it will be an enzyme. *Streptomyces* killer toxin protein also shows structural similarity to Sp-AMP3 based on relationships to MiAMP1 identified with a DALI server search (Holm, 1998) (Fig. 22). These killer toxins exhibit cytocidal effects for both budding and fusion yeasts, which changes the yeast morphology, although the actual target is obscure (Ohki *et al.*, 2001). Another similar protein identified by DALI, the yeast killer toxin secreted by *Williopsis mrakii* (WmKT), has been shown to inhibit β-glucan synthesis, which affects cell wall construction (Antuch *et al.*, 1996).

The combined results suggest an evolutionary relationship among the above-mentioned proteins. We therefore, propose that the residues in the hydrophobic patch on Sp-AMP3 shown in Fig. 19b are involved in β-glucan sugar recognition in this family, and so explain the various proteins action on fungal cell walls.

### 3.3.8 Future perspectives

The protein expression was impossible in bacteria, and is still extremely low in the yeast system, but the results we were able to obtain with the very limited amount of Sp-AMP3 available have in return suggested new avenues worth exploring. Since the protein's ability to bind β-glucan could be the underlying explanation behind the expression problems, we propose to use insect or mammalian cells in future work. If we are able to obtain soluble protein in the quantities needed for crystallization, we will pursue the structures of complexes with β-glucans, as well as extend our studies of other aspects of Sp-AMP function.

# References

Ahlem, C., Huisman, W., Neslund, G. & Dahms, A.S. (1982). Purification and properties of a periplasmic D-xylose-binding protein from *Escherichia coli* K-12. *J Biol Chem* 257(6), 2926-31.

Ames, G.F., Prody, C. & Kustu, S. (1984). Simple, rapid, and quantitative release of periplasmic proteins by chloroform. *J Bacteriol* 160(3), 1181-3.

Anraku, Y. (1968). Transport of sugars and amino acids in bacteria. 3. Studies on the restoration of active transport. *J Biol Chem* 243(11), 3128-35.

Antoniw, J.F., Dunkley, A.M., White, R.F. & Wood, J. (1980). Soluble leaf proteins of virus-infected tobacco (*Nicotiana tabacum*) cultivars [proceedings]. *Biochem Soc Trans* 8(1), 70-1.

Antuch, W., Guntert, P. & Wuthrich, K. (1996). Ancestral beta gamma-crystallin precursor structure in a yeast killer toxin. *Nat Struct Biol* 3(8), 662-5.

Arai, T., Araki, R., Tanaka, A., Karita, S., Kimura, T., Sakka, K. & Ohmiya, K. (2003). Characterization of a cellulase containing a family 30 carbohydrate-binding module (CBM) derived from *Clostridium thermocellum* CelJ: importance of the CBM to cellulose hydrolysis. *J Bacteriol* 185(2), 504-12.

Arakane, Y., Zhu, Q., Matsumiya, M., Muthukrishnan, S. & Kramer, K.J. (2003). Properties of catalytic, linker and chitin-binding domains of insect chitinase. *Insect Biochem Mol Biol* 33(6), 631-48.

Asiegbu, F.O. (2000). Adhesion and development of the root rot fungus (*Heterobasidion annosum*) on conifer tissues: effects of spore and host surface constituents. *FEMS Microbiol Ecol* 33(2), 101-110.

Asiegbu, F.O., Daniel, G. & Johansson, M. (1994). Defense-related reactions of seedling roots of norway spruce to infection by *Heterobasidion annosum* (Fr.) Bref. *Physiological and Molecular Plant Pathology* 45(1), 1-19.

Asiegbu, F.O., Nahalkova, J. & Li, G.S. (2005). Pathogen-inducible cDNAs from the interaction of the root rot fungus *Heterobasidion annosum* with Scots pine (*Pinus sylvestris* L.). *Plant Science* 168(2), 365-372.

Bernier, F. & Berna, A. (2001). Germins and germin-like proteins: Plant do-all proteins. But what do they do exactly? *Plant Physiology and Biochemistry* 39(7-8), 545-554.

Bjorkman, A.J., Binnie, R.A., Zhang, H., Cole, L.B., Hermodson, M.A. & Mowbray, S.L. (1994). Probing protein-protein interactions. The ribose-binding protein in bacterial transport and chemotaxis. *J Biol Chem* 269(48), 30206-11.

Bjorkman, A.J. & Mowbray, S.L. (1998). Multiple open forms of ribose-binding protein trace the path of its conformational change. *J Mol Biol* 279(3), 651-64.

Bol, J.F., Linthorst, H.J.M. & Cornelissen, B.J.C. (1990). Plant Pathogenesis-related proteins induced by virus-Infection. *Annual Review of Phytopathology* 28, 113-138.

Boos, W. (1969). Galactose binding protein and its relationship to beta-methylgalactoside permease from *Escherichia coli*. *European Journal of Biochemistry* 10(1), 66-78.

Boos, W. (1972). Structurally defective galactose-binding protein isolated from a mutant negative in the β-methylgalactoside transport system of *Escherichia coli*. *J Biol Chem* 247(17), 5414-24.

Boos, W. (1974). Bacterial transport. *Annu Rev Biochem* 43(0), 123-46.

Boos, W. (1982). Synthesis of (2R)-glycerol-ortho-beta-D-galactopyranoside by beta-galactosidase. *Methods in Enzymology* 89, 59-64.

Borrok, M.J., Kiessling, L.L. & Forest, K.T. (2007). Conformational changes of glucose/galactose-binding protein illuminated by open, unliganded, and ultra-high-resolution ligand-bound structures. *Protein Sci* 16(6), 1032-41.

Broekaert, W.F., Cammue, B.P.A., DeBolle, M.F.C., Thevissen, K., DeSamblanx, G.W. & Osborn, R.W. (1997). Antimicrobial peptides from plants. *Critical Reviews in Plant Sciences* 16(3), 297-323.

Burstein, C., Cohn, M., Kepes, A. & Monod, J. (1965). Role Du Lactose Et De Ses Produits Metaboliques Dans Linduction De Loperon Lactose Chez *Escherichia coli*. *Biochimica Et Biophysica Acta* 95(4), 634-9.

Chaudhuri, B.N., Ko, J., Park, C., Jones, T.A. & Mowbray, S.L. (1999). Structure of D-allose binding protein from *Escherichia coli* bound to D-allose at 1.8 Å resolution. *J Mol Biol* 286(5), 1519-31.

Cuneo, M.J., Beese, L.S. & Hellinga, H.W. (2008a). Ligand-induced conformational changes in a thermophilic ribose-binding protein. *BMC Struct Biol* 8, 50.

Cuneo, M.J., Tian, Y., Allert, M. & Hellinga, H.W. (2008b). The backbone structure of the thermophilic *Thermoanaerobacter*

*tengcongensis* ribose binding protein is essentially identical to its mesophilic *E. coli* homolog. *BMC Struct Biol* 8, 20.

David, J.D. & Wiesmeyer, H. (1970). Control of xylose metabolism in *Escherichia coli*. *Biochim Biophys Acta* 201(3), 497-9.

Davidson, A.L., Dassa, E., Orelle, C. & Chen, J. (2008). Structure, function, and evolution of bacterial ATP-binding cassette systems. *Microbiol Mol Biol Rev* 72(2), 317-64.

Edreva, A. (2005). Pathogenesis-related proteins: Research progress in the last 15 years. *General and Applied Plant Physiology* 31, 105-124.

Flocco, M.M. & Mowbray, S.L. (1994). The 1.9 Å X-ray structure of a closed unliganded form of the periplasmic glucose/galactose receptor from *Salmonella typhimurium*. *J Biol Chem* 269(12), 8931-6.

Gilkes, N.R., Henrissat, B., Kilburn, D.G., Miller, R.C., Jr. & Warren, R.A. (1991). Domains in microbial beta-1,4-glycanases: sequence conservation, function, and enzyme families. *Microbiol Rev* 55(2), 303-15.

Gilson, E., Alloing, G., Schmidt, T., Claverys, J.P., Dudler, R. & Hofnung, M. (1988). Evidence for high-affinity binding-protein dependent transport-systems in gram-positive bacteria and in *Mycoplasma*. *Embo Journal* 7(12), 3971-3974.

Higgins, C.F. (1992). ABC transporters: from microorganisms to man. *Annu Rev Cell Biol* 8, 67-113.

Higgins, C.F., Hyde, S.C., Mimmack, M.M., Gileadi, U., Gill, D.R. & Gallagher, M.P. (1990). Binding protein-dependent transport systems. *J Bioenerg Biomembr* 22(4), 571-92.

Holm, L. (1998). Unification of protein families. *Curr Opin Struct Biol* 8(3), 372-9.

Iseli, B., Boller, T. & Neuhaus, J.M. (1993). The N-terminal cysteine-rich domain of tobacco class I chitinase is essential for chitin binding but not for catalytic or antifungal activity. *Plant Physiol* 103(1), 221-6.

Kalckar, H.M. (1971). The periplasmic galactose binding protein of *Escherichia coli*. *Science* 174(9), 557-65.

Karlsson, M., Olson, A. & Stenlid, J. (2003). Expressed sequences from the basidiomycetous tree pathogen *Heterobasidion annosum* during early infection of Scots pine. *Fungal Genetics and Biology* 39(1), 51-59.

Kleywegt, G.J. & Jones, T.A. (1997). Detecting folding motifs and similarities in protein structures. *Methods Enzymol* 277, 525-45.

Korhonen, K., Bobko, I., Hanso, S., Piri, T. & Vasiliauskas, A. (1992). Intersterility groups of *Heterobasidion annosum* in some spruce and pine stands in Byelorussa, Lithuania and Estonia. *European Journal of Forest Pathology* (22), 384-391.

Lam, V.M., Daruwalla, K.R., Henderson, P.J. & Jones-Mortimer, M.C. (1980). Proton-linked D-xylose transport in *Escherichia coli*. *J Bacteriol* 143(1), 396-402.

Lin, E.C.C. (1987). Dissimilation pathways for sugars, polyols, and carboxlates. . *In: Escherichia coli and Salmonella typhimurium: Cellular and Molecular Biology (Neidhart, F. C., Ingraham, J. L., Low, K. B., Magasanik, B., Schaechter, M. and Umbarger, H. E. Eds.)*, 244-84.

Linthorst, H.J.M. (1991). Pathogenesis-related proteins of plants. *Critical Reviews in Plant Sciences* 10(2), 123-150.

Lokman, B.C., Leer, R.J., van Sorge, R. & Pouwels, P.H. (1994). Promoter analysis and transcriptional regulation of *Lactobacillus pentosus* genes involved in xylose catabolism. *Mol Gen Genet* 245(1), 117-25.

Magnusson, U., Chaudhuri, B.N., Ko, J., Park, C., Jones, T.A. & Mowbray, S.L. (2002). Hinge-bending motion of D-allose-binding protein from *Escherichia coli*: three open conformations. *J Biol Chem* 277(16), 14077-84.

McManus, A.M., Nielsen, K.J., Marcus, J.P., Harrison, S.J., Green, J.L., Manners, J.M. & Craik, D.J. (1999). MiAMP1, a novel protein from *Macadamia integrifolia* adopts a Greek key beta-barrel fold unique amongst plant antimicrobial proteins. *J Mol Biol* 293(3), 629-38.

Miller, D.M., 3rd, Olson, J.S., Pflugrath, J.W. & Quiocho, F.A. (1983). Rates of ligand binding to periplasmic proteins involved in bacterial transport and chemotaxis. *J Biol Chem* 258(22), 13665-72.

Miller, D.M., Olson, J.S. & Quiocho, F.A. (1980). The mechanism of sugar binding to the periplasmic receptor for galactose chemotaxis and transport in *Escherichia coli*. *Journal of Biological Chemistry* 255(6), 2465-2471.

Mowbray, S.L. & Petsko, G.A. (1983). The X-Ray structure of the periplasmic galactose binding-protein from *Salmonella typhimurium* at 3.0Å resolution. *Journal of Biological Chemistry* 258(13), 7991-7997.

Mowbray, S.L., Smith, R.D. & Cole, L.B. (1990). Structure of the periplasmic glucose/galactose receptor of *Salmonella typhimurium*. *Receptor* 1(1), 41-53.

Murshudov, G.N., Vagin, A.A. & Dodson, E.J. (1997). Refinement of macromolecular structures by the maximum-likelihood method. *Acta Crystallographica Section D-Biological Crystallography* 53, 240-255.

Murzin, A.G., Brenner, S.E., Hubbard, T. & Chothia, C. (1995). SCOP: a structural classification of proteins database for the investigation of sequences and structures. *J Mol Biol* 247(4), 536-40.

Nakanishi, N., Shneider, N.A. & Axel, R. (1990). A family of glutamate receptor genes: evidence for the formation of heteromultimeric receptors with distinct channel properties. *Neuron* 5(5), 569-81.

Ohki, S.Y., Kariya, E., Hiraga, K., Wakamiya, A., Isobe, T., Oda, K. & Kainosho, M. (2001). NMR structure of *Streptomyces* killer toxin-like protein, SKLP: further evidence for the wide distribution of

single-domain beta gamma-crystallin superfamily proteins. *J Mol Biol* 305(1), 109-20.

Park, J.E., Park, C.J., Sakchaisri, K., Karpova, T., Asano, S., McNally, J., Sunwoo, Y., Leem, S.H. & Lee, K.S. (2004). Novel functional dissection of the localization-specific roles of budding yeast polo kinase Cdc5p. *Mol Cell Biol* 24(22), 9873-86.

Piri, T. (1998). Effects of vitality fertilization on the growth of *Heterobasidion annosum* in Norway spruce roots. *European Journal of Forest Pathology* 28(6), 391-397.

Quiocho, F.A. (1990). Atomic structures of periplasmic binding proteins and the high-affinity active transport systems in bacteria. *Philos Trans R Soc Lond B Biol Sci* 326(1236), 341-51.

Quiocho, F.A. & Vyas, N.K. (1984). Novel stereospecificity of the L-arabinose-binding protein. *Nature* 310(5976), 381-6.

Raikhel, N.V., Lee, H.I. & Broekaert, W.F. (1993). Structure and function of chitin-binding proteins. *Annual Review of Plant Physiology and Plant Molecular Biology* 44, 591-615.

Read, R.J. (1986). Improved Fourier coefficients for maps using phases from partial structures with errors. *Acta Crystallographica Section A* 42, 140-149.

Reeves, R.E. (1951). Cuprammonium-glycoside complexes. *Adv Carbohydr Chem* 6, 107-34.

Rotman, B., Ganesan, A.K. & Guzman, R. (1968). Transport systems for galactose and galactosides in *Escherichia coli*. II. Substrate and inducer specificities. *J Mol Biol* 36(2), 247-60.

Ryals, J.A., Neuenschwander, U.H., Willits, M.G., Molina, A., Steiner, H.Y. & Hunt, M.D. (1996). Systemic Acquired Resistance. *Plant Cell* 8(10), 1809-1819.

Sack, J.S., Saper, M.A. & Quiocho, F.A. (1989). Periplasmic binding protein structure and function. Refined X-ray structures of the leucine/isoleucine/valine-binding protein and its complex with leucine. *J Mol Biol* 206(1), 171-91.

Sastry, P.S. & Kates, M. (1964). Lipid components of leaves. V. galactolipids, cerebrosides, and lecithin of runner-bean leaves. *Biochemistry* 3, 1271-80.

Shamanna, D.K. & Sanderson, K.E. (1979b). Genetics and regulation of D-xylose utilization in *Salmonella typhimurium* LT2. *J Bacteriol* 139(1), 71-79.

Shilton, B.H. (2008). The dynamics of the MBP-MalFGK(2) interaction: a prototype for binding protein dependent ABC-transporter systems. *Biochim Biophys Acta* 1778(9), 1772-80.

Shuman, H.A. (1982). Active transport of maltose in *Escherichia coli* K-12. Role of the periplasmic maltose-binding protein and evidence for a substrate recognition site in the cytoplasmic membrane. *J Biol Chem* 257(10), 5455-61.

50

Song, S. & Park, C. (1997). Organization and regulation of the D-xylose operons in *Escherichia coli* K-12: XylR acts as a transcriptional activator. *J Bacteriol* 179(22), 7025-32.

Sooriyaarachchi, S., Ubhayasekera, W., Boos, W. & Mowbray, S.L. (2009). X-ray structure of glucose/galactose receptor from *Salmonella typhimurium* in complex with the physiological ligand, (2R)-glyceryl-beta-D-galactopyranoside. *Febs J* 276(7), 2116-24.

Tam, R. & Saier, M.H., Jr. (1993). Structural, functional, and evolutionary relationships among extracellular solute-binding receptors of bacteria. *Microbiol Rev* 57(2), 320-46.

Tang, C., Schwieters, C.D. & Clore, G.M. (2007). Open-to-closed transition in apo maltose-binding protein observed by paramagnetic NMR. *Nature* 449(7165), 1078-82.

Vagin, A. & Teplyakov, A. (1997). MOLREP: an automated program for molecular replacement. *Journal of Applied Crystallography* 30, 1022-1025.

van Loon, L.C. (1999). Occurrence and properties of plant pathogenesis-related proteins. In pathogenesis-related proteins in plants. *(Muthukrishnan S, ed, pp. 1-19. CRC Press.*

van Loon, L.C., Pierpoint, W.S., Boller, T. & Conejero, V. (1994). Recommendations for naming plant pathogenesis-related proteins. *Plant Mol Biol Rep* 12, 245-264.

van Loon, L.C. & van Strien, E.A. (1999). The families of pathogenesis-related proteins, their activities, and comparative analysis of PR-1 type proteins. *Physiol. Mol. Plant Pathol* 55, 85-97.

Vyas, M.N., Vyas, N.K. & Quiocho, F.A. (1994). Crystallographic analysis of the epimeric and anomeric specificity of the periplasmic transport/chemosensory protein receptor for D-glucose and D-galactose. *Biochemistry* 33(16), 4762-8.

Vyas, N.K., Vyas, M.N. & Quiocho, F.A. (1983). The 3 Å resolution structure of a deuterium-galactose-binding protein for transport and chemotaxis in *Escherichia coli*. *Proceedings of the National Academy of Sciences of the United States of America-Biological Sciences* 80(7), 1792-1796.

Vyas, N.K., Vyas, M.N. & Quiocho, F.A. (1987). A novel calcium-binding site in the galactose-binding protein of bacterial transport and chemotaxis. *Nature* 327(6123), 635-638.

Vyas, N.K., Vyas, M.N. & Quiocho, F.A. (1988). Sugar and signal-transducer binding sites of the *Escherichia coli* galactose chemoreceptor protein. *Science* 242(4883), 1290-5.

Weenink, R.O. (1961). Acetone-soluble lipids of grasses and other forage plants .1. Galactolipids of red clover (*Trifolium Pratense*) leaves. *Journal of the Science of Food and Agriculture* 12(1), 34-&.

Wilson, D.B. (1974). Source of energy for the *Escherichia coli* galactose transport systems induced by galactose. *J Bacteriol* 120(2), 866-71.

Zou, J.Y., Flocco, M.M. & Mowbray, S.L. (1993). The 1.7 Å refined X-ray structure of the periplasmic glucose/galactose receptor from *Salmonella typhimurium. J Mol Biol* 233(4), 739-52.

# Acknowledgments

*I wish to express my sincere gratitude to my supervisor Sherry Mowbray, for offering me a position in her lab in the first place, and for the constant support and encouragement. Thanks for the risk you have taken by having a student without any background knowledge and listening to her very carefully and being so patient! Hope I haven't disappointed you (that much)! At the same time I am deeply indebted to my second supervisor Wimal Ubhayasekera for his initial stimulus, selfless guidance, advice and encouragement throughout the period of this study as well as in the successful completion of the thesis. Sorry …for the disturbances I made numerous times asking questions. Thank you for all your efforts! I would like to thank Frederick O. Asiegbu for his supervision, and for making me feel welcome in his research group.*

*Adrian, You were the saviour when I lost myself in the lab without knowing where I should start and what should I do! Thanks a lot, Adrian, you always encouraged me, helped me and never said, "go back and come later" … even when you were busy writing your thesis in the last moments…. Thanks for each piece of advice and each minute you spent to find out answers for my problems. ….. AMP still challenges us  ..but we are going to win soon!*

*I also would like to thank……*

*Alwyn Jones for the always extended helpful hand whenever I got stuck with "O" and also Lars Liljas for the X-ray crystallography course.*

*Tex, the crystallization guru in the lab, you always had suggestions for my problems. They really worked. Jerry.. for all the brilliant ideas and the advice about my projects*

*Christer and Erling, for keeping the computers running and always having time for me when I have problems with them, Elleonor, Stefan. Inger, Ulla and Margareta for all the administrative help. Thank you Mark, you always helped me whenever I was having difficulties with Molscript and Molray!*

*Many thanks to the @xray group, all the past and present members. Thanks a lot for your co-operation and assistance in numerous ways whenever it was needed. Even a single smile from you helped me to survive in the lab.*

*Ulf, it is my pleasure to thank you for your support with the mass spec. It is a pity that we could not manage to have crystals for those projects.  Sophia, you were so kind and always had time for me. I am happy that I know you! ….this ribose binding confused us, didn't it?*

*Mee-Len Chye, in your lab I became skilled in many techniques, and I am happy to pay my gratitude! Sharon, I was lucky to have your enduring assistance during the period in Hong Kong. Thank you a lot!*

*Iva, my best friend in Sweden, thanks for all the moments we shared together, it was really nice to listen to you!*

*My gratitude is extended to all the people from my motherland who live in Uppsala, for all the moments we have shared together, and the remembrance you bring about Sri Lanka!*

*I am also extremely grateful to my dearest sister and brother for helping me in every way to complete this piece of work successfully. I missed you two all the time.*

*My loving mother and father, your endless love, guidance, stimulations brought me this far. Your care and support were the ultimate energy to my journey in education. I am who I am because of you!*

*Finally I must say that I am an outcome of Sri Lanka's free education system. I sincerely bow my head towards my nation in thanks. The education and experience I gained in Sweden is highly appreciated.*

*Sanjee*                                                     *June, 2010*